Program Digest, 2019 IEEE International Ultrasonics Symposium (IUS)
Glasgow, Scotland, October 6-9, 2019

Full 3D FEM Analysis of Scattering at a Border Between IDT and Reflector in SAW Resonators

Akihiro Iyama[1], Xinyi Li[2,1], Jingfu Bao[2], Naoto Matsuoka[3,1], Tatsuya Omori[1] and Ken-ya Hashimoto[1,2]
[1]*Graduate School of Science and Technology Chiba University, Chiba, Japan*
[2]*School of Electronic Engineering University of Electronic Science and Technology of China, Chengdu, China*
[3]*Nihon Dempa Kogyo Co., Ltd., Tokyo, Japan*

***Abstract*— This paper describes 3D FEM simulation of scattering at a border between IDT and reflector in SAW resonators using hierarchical cascading technique and general purpose graphic processing unit. SH-type SAW on the 42°YX-$LiTaO_3$ substrate is chosen. It is shown how the reflector design affects the scattering loss at the border. It is also shown that scattering fields can be observed selectively by the use of the wavenumber domain analysis.**

Index Terms*—*SAW; FEM; scattering; hierarchical cascading

I. Introduction

Much effort has been paid for loss reduction of SAW resonators, and it was shown that very high *Q* SAW devices can be mass-produced by using a very thin single crystal $LiTaO_3$ plate bonded to a Si or quartz substrate[1-4]. Nevertheless, it is believed that unknown and non-intrinsic loss mechanism(s) still remain.

One candidate is a SAW scattering at a border between the IDT and reflector. Even when their grating designs are identical, their bus-bars are separated to each other, and gaps are necessary between bus-bars and grating fingers only in the IDT. However, there was no way to analyze SAW scattering at the border theoretically, and the gaps was designed empirically. Although the full 3D analysis is necessary to study influence of the gaps, it was believed not practical for SAW devices until very recent because of required computer power.

Koskela, et al. proposed the hierarchical cascading technique (HCT) for drastic acceleration of the finite element method (FEM) analysis of SAW devices mainly composed of periodic structures[5]. Solal, et al. showed that HCT makes the full 3D simulation possible[6]. The authors' group also showed that the high-end general purpose graphic processing unit (GPGPU) enables further speed up of the HCT-based FEM simulation[7,8]. The acceleration becomes more significant with larger model size, and the full 3D simulation can be executed in surprising speed although applicable model size is limited by the memory size (32 GB) embedded in current GPGPU.

This paper describes full 3D analysis of SAW scattering at a border between IDT and reflector regions by HCT-based FEM with GPGPU acceleration. Synchronous one-port SAW resonators on 42°YX-$LiTaO_3$[9] are used for the discussion. It is shown how the reflector design affects the scattering loss at the border. It is also shown that scattering fields can be observed selectively by the use of the wavenumber domain analysis[10].

II. 3D Hierarchical Cascading

First, the whole simulation model is decomposed into small unit blocks (See Fig. 1). The FEM matrix of each unit block is rearranged as

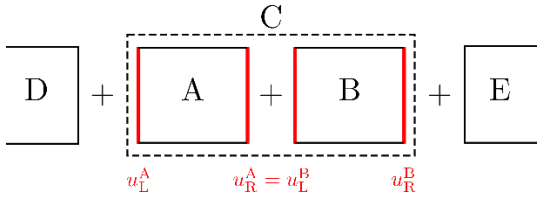

Fig. 1 Cascading two unit blocks

$$\begin{bmatrix} A_{LL} & A_{LI} & 0 & A_{LV} \\ A_{IL} & A_{II} & A_{IR} & A_{IV} \\ 0 & A_{RR} & A_{RI} & A_{RV} \\ A_{VL} & A_{VI} & A_{VR} & A_{VV} \end{bmatrix} \begin{bmatrix} u_L \\ u_I \\ u_R \\ V \end{bmatrix} = \begin{bmatrix} T_L \\ 0 \\ T_R \\ -q \end{bmatrix}, \quad (1)$$

where A_{ij} are sub-matrices, and u, T, and q are displacements (DOFs), stress, electric charge on the electrode, respectively. Subscripts R, L, and I indicate values at left boundary (L), the right boundary (R), and interior (I), respectively, of the unit block, and the subscript V indicates the value related to the electric potential V, respectively. Elimination of u_R reduces Eq. (1) to the following B-matrix:.

$$\begin{bmatrix} B_{LL} & B_{LR} & B_{LV} \\ B_{RL} & B_{RR} & B_{RV} \\ B_{VL} & B_{VR} & B_{VV} \end{bmatrix} \begin{bmatrix} u_L \\ u_R \\ V \end{bmatrix} = \begin{bmatrix} T_L \\ T_R \\ -q \end{bmatrix}. \quad (2)$$

When two blocks A and B in Fig. 1 are identical, the B-matrix after their cascading is given by

$$\begin{bmatrix} B_{LL} & B_{LR} & 0 & B_{LV} \\ B_{RL} & B_{RR}+B_{LL} & B_{LR} & B_{LV} \pm B_{RV} \\ 0 & B_{RL} & B_{RR} & \pm B_{RV} \\ B_{VL} & B_{VR} \pm B_{VL} & \pm B_{VR} & 2B_{VV} \end{bmatrix} \begin{bmatrix} u_L^A \\ u_R^A (=u_L^B) \\ u_R^B \\ V \end{bmatrix} = \begin{bmatrix} T_L^A \\ 0 \\ T_R^B \\ -q \end{bmatrix} \quad (3)$$

because $u_R{}^A = u_L{}^B$ and $T_R{}^A + T_L{}^B = 0$. In the equation, the superscripts A and B indicate values in blocks A and B, respectively, and "±" is the polarity of the applied voltage in the unit B relative to that in the unit A. Since Eq. (3) has the same form as Eq. (1), Eq. (3) can be reduced into the same form of

Eq. (2). Application of this procedure between the newly generated B matrices, we can obtain the B matrix for cascading four (2^2) blocks. Then run time for the B matrix calculation increases by N when identical blocks are cascaded for 2^N times. Thus the simulation target includes a lot of identical blocks like SAW devices, HCT can accelerate the FEM calculation significantly.

Originally HCT was applied to periodically aligned grating structures[5]. Here HCT is also applied to the thickness and aperture directions for speed up. Finally, the B matrices for various elements are cascaded, and the whole structure is analyzed using the boundary conditions at the outermost edges.

III. Simulation Model

Fig.1 shows the simulation model of a SAW resonator. The symmetry boundary condition is applied to the center of the IDT while the perfect matching layer (PML) is applied to both the bottom surface and side walls of the 42°YX-$LiTaO_3$ substrate.

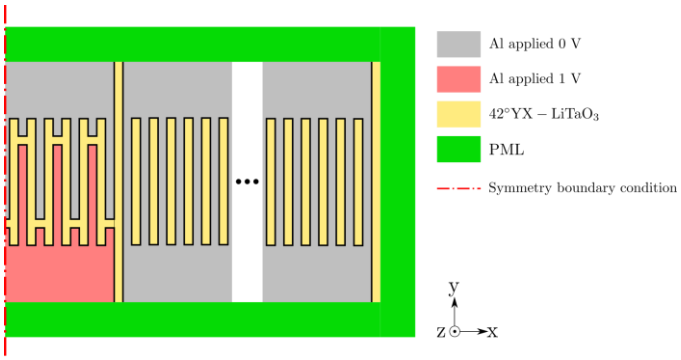

Fig. 1. A simulation model of a SAW resonator (top view).

Table I shows the structural parameters used in the following simulation. The number of IDT electrodes is set small intensively while that of reflector electrodes is set extremely large to emphasize influence of the border design. Note that the calculation time is not so dependent of the number of electrodes[8].

Table I. Design parameters of IDT region

Substrate	42°YX-$LiTaO_3$
Wavelength λ	4 μm
Al thickness	0.08λ
Metallization ratio	0.5
Aperture W	10λ
Number of IDT electrodes	33
Gap length	0.5λ
Dummy electrode length	1λ
Bas-bar width	Infinite (terminated by PML)

Fig. 2 shows three types of reflector designs discussed in this paper: Normal, Reflector A, and Reflector B. The normal one is most popular, while Reflector A is the same structure as IDT so as to avoid the discontinuity between IDT and reflector. Note two electrodes are electrically grounded. Reflector B is a trial to avoid abrupt variation of the gap length.

The following calculations were performed by Intel Xeon W-2123 and NVIDIA GV100 as a central processing unit and GPGPU, respectively. Execution time for each frequency point was circa 200 sec. excluding image processing.

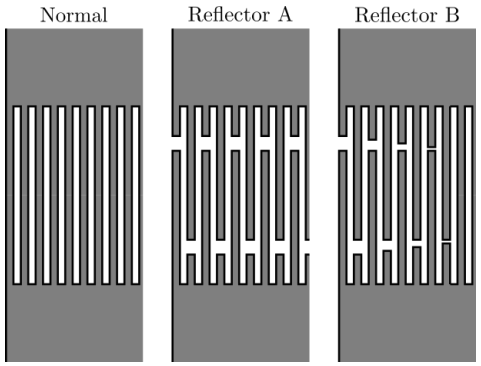

Fig. 2. Three types of reflector designs.

IV. SAW Scattering Analysis

A. Frequency response

Fig. 3 shows variation of calculated conductance G of the resonator with reflector designs. The resonance and anti-resonance frequencies are 985 MHz and 1011 MHz, and scarcely changed with the reflector design. It is seen that the design A offers better Q than the normal one at frequencies less than 992 MHz while Q becomes worse above the frequency. Reflector B gives a cross between these two results.

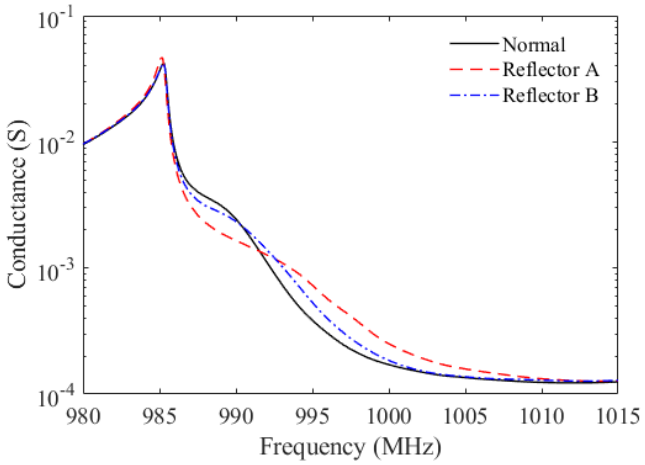

Fig. 3. Variation of the calculated conductance of SAW resonators with reflector design.

B. Wavenumber domain analysis

Since the SAW scattering at edges is tiny, it is hard to observe it from the calculated SAW field directly.

Fig. 4 shows the wavenumber (β_x-β_y) domain spectrum of the calculated displacement on the substrate surface at 995 MHz.

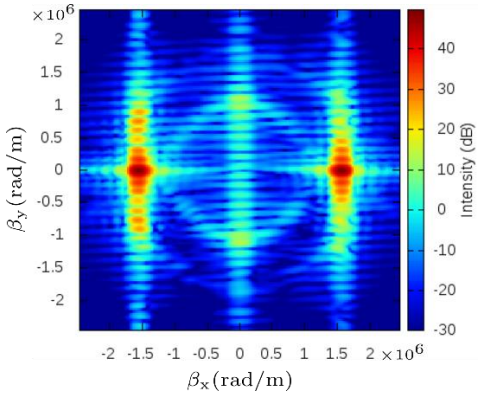

Fig. 4. Wavenumber (β_x-β_y) domain spectrum of the calculated displacement at 995 MHz when the normal reflector is employed.

Two bright spots on the β_x axis are due to eigen (SAW) modes resonating in the structure. Small peaks nearby are artifacts (sidelobes) caused by the numerical processing. Two circles are also seen, and they correspond to scattered and not-guided acoustic wave fields. From their radius, inner and outer circles are identified as longitudinal and shear waves. We cannot judge whether they are surface or bulk acoustic waves only from this result.

Two spots are also seen on the β_y axis. It indicates existence of eigen (SAW) modes propagating to the ±y directions.

Next, two window functions shown in Fig. 5 were prepared for selective observation of the scattered field in the space (*x*-*y*) domain. Windows 1 and 2 are for outer and inner circles, respectively, in Fig. 4. After truncation by these functions, 2D inverse FFT is applied to convert data in the β_x-β_y domain to the *x*-*y* one.

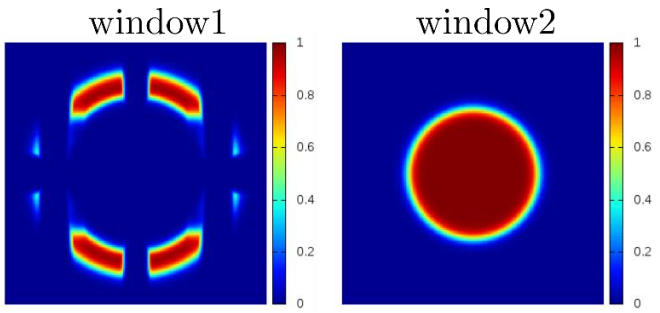

Fig. 5. Window functions for selective observation of the scattered field.

Figs. 6(a) and (b) show the results of IFFT with window 1 at 988 MHz and 995 MHz, respectively. It is seen that strong scattering occurs at the border between the gap region of the IDT and the reflector. The normal one is the strongest, and the others are much weaker. In this case, scattering properties seem almost independent of the frequency.

Fig. 7(a) and (b) show the results of IFFT with window 2 at 988 MHz and 995 MHz, respectively. Strong scattering can be seen at the gaps in the IDT region and reflector regions.

At 988 MHz, the intensity is exceptionally weak for the reflector A in the gap regions of not only the reflector but also the IDT. This means the bright fields in the gap region are mainly caused by the reflective scattering at the boundary. This is because excited SAW field is considered to be almost independent of the reflector design.

In contrast, the intensity is large for all cases at 995 MHz. This means that it is caused by the scattering of propagating SAWs.

It is well known that the gaps cause SAW attenuation in this substrate and their influence becomes significant at frequencies close to the anti-resonance[6]. These facts explain these results.

It is also known that they can be reduced by minimizing the gap length[8]. We also performed the same calculation for the identical structure with different gap lengths, and variation of the SAW scattering was clearly observed at 995 MHz.

V. Conclusion

This paper described 3D HCT-based FEM simulation of SAW scattering at a border between IDT and reflector in SAW resonators on the Al/42°YX-$LiTaO_3$ using GPGPU. As a demonstration, SAW resonators with three types of reflector designs were analyzed.

It was shown that the reflector design affects the loss of SAW resonators. Based on the wavenumber domain analysis, two loss mechanisms at the gap region were identified.

References

[1] T. Takai, H. Iwamoto, Y. Takamine, H. Yamazaki, T. Fuyutsume, H. Kyoya, T. Nakao, H. Kando, M. Hiramoto, T. Toi, M. Koshino, and N. Nakajima, "High-performance SAW resonator on new multilayered substrate using $LiTaO_3$ crystal," IEEE Trans. Ultrason., Ferroelectr., Freq. Contr., **64**, 9, 2017, pp. 1382-1389.

[2] T. Takai, H. Iwamoto, Y. Takamine, T. Fuyutsume, T. Nakao, M. Hiramoto, T. Toi, and M. Koshino, "High-performance SAW resonator with simplified $LiTaO_3/SiO_2$ double layer structure on Si Substrate," IEEE Trans. Ultrason., Ferroelectr., Freq. Contr., **66**, 5, 2019, pp. 1006-1013.

[3] M. Kadota and S. Tanaka, "Near-Zero TCF of HAL SAW resonator with $LiTaO_3$-on-Quartz structure," in Proc. IEEE Freq. Cont. Symp., 2018, 10.1109/fcs.2018.8597496

[4] S. Inoue and M. Solal, "Spurious free SAW resonators on layered substrate with ultra-high Q, high coupling and small TCF," in Proc. IEEE Ultrason. Symp., 2018, 10.1109/ultsym.2018.8579852

[5] J. Koskela, P.Maniadis, B.A.Willemsen, P.Turner, R.B.Hammond, N.O.Fenzi, and V.Plessky, "Hierarchical cascading in 2D FEM simulation of finite SAW devices with periodic block structure," in Proc. IEEE Ultrason. Symp., 2016, 10.1109/ultsym.2016.7728574

[6] M. Solal, M. Gallagher and A.Tajic, "Full 3D simulation of SAW resonators using hierarchical cascading FEM," in Proc. IEEE Ultrason. Symp., 2017, 10.1109/ultsym.2017.8092166

[7] X.Li, J.Bao, Y.Huang, B.F.Zhang, T.Omori, and K.Hashimoto, "Use of Hierarchical Cascading Technique for FEM Analysis of Transverse Mode Behaviors in Surface Acoustic Wave Devices," IEEE Trans. Ultrason., Ferroelec., and Freq. Contr., **67** (2019) [early access] 10.1109/TUFFC.2019.2932105

[8] X. Li, J.Bao, L.Qiu, N.Matsuoka, T.Omori and K. Hashimoto, "3D FEM simulation of SAW resonators using hierarchical cascading technique and general purpose graphic processing unit," Japanese Journal of Applied Physics, **58**, 7, SGGC05, 2019.

[9] O.Kawachi, S.Mineyoshi, G.Endoh, M.Ueda, O.Ikata, K.Hashimoto and M.Yamaguchi, "Optimal Cut for Leaky SAW on $LiTaO_3$ for High Performance Resonators and Filters," IEEE Trans. Ultrason., Ferroelec., and Freq. Contr., **48**, 5 (2001) pp. 1442-1448.

[10] K.Hashimoto, H.Kamizuma, M.Watanabe, T.Omori and M.Yamaguchi, "Wavenumber Domain Analysis of Two-Dimensional SAW Images Captured by Phase-Sensitive Laser Probe System," IEEE Trans. Ultrason., Ferroelec., and Freq. Contr., **54**, 5 (2007) pp. 1072-1075.

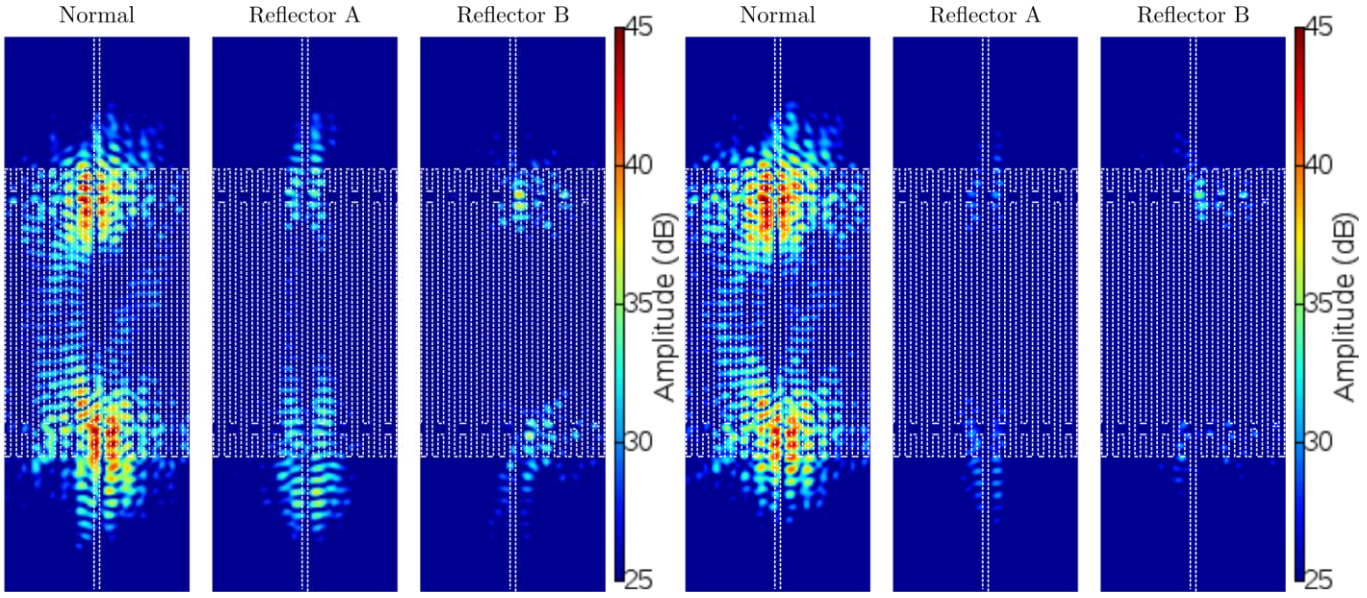

(a). 988 MHz (b). 995 MHz

Fig. 6. Results of IFFT with window1 (white broken line is electrodes pattern).

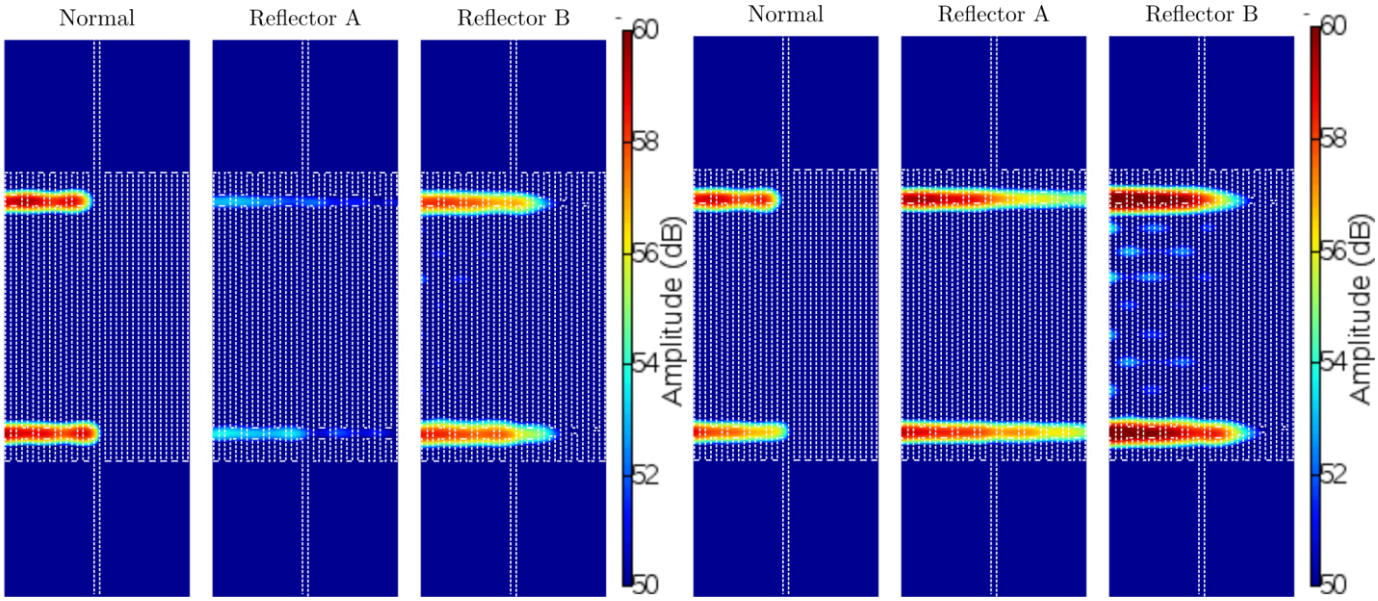

(a). 988 MHz (b). 995 MHz

Fig. 7. Results of IFFT with window2 (white broken line is electrodes pattern).